Article:
Miele, L, Evans, RML, Cunniffe, NJ et al. (2 more authors) (2023) Evolutionary Epidemiology Consequences of Trait-Dependent Control of Heterogeneous Parasites. The American Naturalist, 202 (5). E130-E146. ISSN 0003-0147

https://doi.org/10.1086/726062

E-Article

Evolutionary Epidemiology Consequences of Trait-Dependent Control of Heterogeneous Parasites

Leonardo Miele,[1,2,*] R. M. L. Evans,[1] Nik J. Cunniffe,[3] Clara Torres-Barceló,[4] and Daniele Bevacqua[2]

1. School of Mathematics, University of Leeds, Leeds LS2 9JT, United Kingdom; 2. INRAE, UR1115 Plantes et Systèmes de culture Horticoles (PSH), Site Agroparc, 84914 Avignon, France; 3. Department of Plant Sciences, University of Cambridge, Cambridge, United Kingdom; 4. INRAE, Pathologie Végétale, F-84140, Montfavet, France

Submitted February 14, 2022; Accepted May 5, 2023; Electronically published October 5, 2023

Online enhancements: supplemental PDF.

ABSTRACT: Disease control can induce both demographic and evolutionary responses in host-parasite systems. Foreseeing the outcome of control therefore requires knowledge of the eco-evolutionary feedback between control and system. Previous work has assumed that control strategies have a homogeneous effect on the parasite population. However, this is not true when control targets those traits that confer to the parasite heterogeneous levels of resistance, which can additionally be related to other key parasite traits through evolutionary trade-offs. In this work, we develop a minimal model coupling epidemiological and evolutionary dynamics to explore possible trait-dependent effects of control strategies. In particular, we consider a parasite expressing continuous levels of a trait-determining resource exploitation and a control treatment that can be either positively or negatively correlated with that trait. We demonstrate the potential of trait-dependent control by considering that the decision maker may want to minimize both the damage caused by the disease and the use of treatment, due to possible environmental or economic costs. We identify efficient strategies showing that the optimal type of treatment depends on the amount applied. Our results pave the way for the study of control strategies based on evolutionary constraints, such as collateral sensitivity and resistance costs, which are receiving increasing attention for both public health and agricultural purposes.

Keywords: trade-offs, mathematical modeling, evolutionary epidemiology, disease management, heterogeneous pathogens, trait-structured populations.

Introduction

Disease and pest control strategies aim to eradicate or mitigate the exploitation of a parasite population on a host population of economic (agriculture) or public health (humans) interest (Gilligan 2002). By altering the ecological host-parasite interactions, a control strategy can induce both demographic effects (Gilligan and van den Bosch 2008) and evolutionary responses (Day et al. 2020). Predicting the outcome of control strategies in a system therefore depends on our understanding of its eco-evolutionary feedbacks (Day and Gandon 2006), that is, on the evolutionary epidemiology behavior (Galvani 2003).

In addition to experimental studies, theoretical work based on evolutionary epidemiology has provided insights into control strategies and on their (often counterintuitive) consequences. For instance, host reduction (e.g., via culling) may increase disease abundance and prevalence (Bolzoni and De Leo 2013); altering parasite growth, such as in vaccination campaigns, can lead to selection for more virulent parasites, thus increasing disease severity (Gandon et al. 2001, 2003; Zurita-Gutiérrez and Lion 2015). Studies of the emergence and spread of multidrug resistance have also shown that the efficacy of a control strategy may depend on the structure of the host population (e.g., age or spatial distributions) as well as on parasite heterogeneity (Blanquart et al. 2018; Lehtinen et al. 2019; McLeod and Gandon 2021). Furthermore, models also provide a low-cost tool to explore and optimize large-scale agricultural practices (Rimbaud et al. 2018), such as the deployment of disease-resistant cultivars (Taylor and Cunniffe 2022) and crop rotation (Bargués-Ribera and Gokhale 2020), whose in-field implementation can consume considerable time and resources.

Most of the experimental and theoretical work has assumed that control strategies have a homogeneous effect on parasites or that parasites are endowed with a genetically

* Corresponding author; email: mieleo91@gmail.com.

ORCIDs: Miele, https://orcid.org/0000-0002-5019-0469; Evans, https://orcid.org/0000-0003-4172-8455; Cunniffe, https://orcid.org/0000-0002-3533-8672; Torres-Barceló, https://orcid.org/0000-0003-2116-1471; Bevacqua, https://orcid.org/0000-0002-3341-1696.

  https://doi.org/10.1086/726062

encoded resistance that is either present or absent (qualitative resistance; REX Consortium 2010). However, this picture neglects the cases where the efficacy of a treatment depends on quantitative traits that can be heterogeneously expressed in the parasite population (quantitative resistance; Corwin and Kliebenstein 2017). In fact, parasites have developed several defense mechanisms that can quantitatively affect drug uptake, leading to variable levels of resistance (Munita and Arias 2016; El Meouche and Dunlop 2018). Widespread examples of such mechanisms are metabolic regulators (Chebotar et al. 2021), biofilms (Costerton et al. 1999; Fanning and Mitchell 2012), efflux pumps (Martinez et al. 2009), flagella (Lyu et al. 2021), and capsules (Song et al. 2021). Thus, a parasite population will often exhibit heterogeneity in the expression of key traits (Hewitt et al. 2016; González et al. 2019; Perrier et al. 2019; Schröter and Dersch 2019; Dutta et al. 2020), potentially leading to heterogeneous trait-dependent treatment effects (Porco et al. 2005; Laine and Barrès 2013; Martínez et al. 2019; Alizon 2020) and ultimately threatening the control strategy's overall efficacy (Gefen and Balaban 2009; Patyka et al. 2016; Weigel and Dersch 2018; Dewachter et al. 2019).

The occurrence of trait-dependent treatment effects is expected to be exacerbated in the future, as many of the new promising strategies to counter resistance escalation are based on the exploitation of trait-specific evolutionary constraints (Palmer and Kishony 2013; Lässig et al. 2017; Furusawa et al. 2018), such as fitness costs of resistance (Lenski 1998; Andersson and Hughes 2010; Vincent et al. 2013; Hawkins and Fraaije 2018), life history (Shoval et al. 2012), and metabolic (Weiße et al. 2015; Pinheiro et al. 2021) trade-offs and collateral sensitivity (Lázár et al. 2018; Barbosa et al. 2019; Maltas and Wood 2019; Maeda et al. 2020; Roemhild and Andersson 2021). For instance, bacterial efflux pumps rely on proton motive force both to import some toxic compounds (e.g., aminoglycosides; Taber et al. 1987; Alekshun and Levy 2007) and to expel others (e.g., β-lactams; Okusu et al. 1996; Lázár et al. 2013; Suzuki et al. 2014); therefore, strains with a reduced proton motive force will be more resistant to one antibiotic but more sensitive to the other—and vice versa (Pál et al. 2015; Roemhild and Andersson 2021). This phenomenon is a textbook example of antibiotic collateral sensitivity, but it also affects other types of control strategies, such as fungicides, copper use, and phage therapy, and it can potentially involve other fields of application, such as biocontrol methods in agriculture.

Phage therapy employs viruses (phages) that selectively attack bacteria and ultimately kill them. It has been observed that resistance to both phages and antibiotics is often costly for bacteria (Meaden et al. 2015; Mangalea and Duerkop 2020; Laure and Ahn 2022): selection pressure often leads to the evolution of bacterial strains that are resistant to either phage or antibiotic therapy, which can therefore be applied in combination to obtain synergistic antimicrobial effects (Torres-Barceló and Hochberg 2016; Coyne et al. 2022; Kebriaei et al. 2022). In addition, recently discovered phages targeting mechanisms involved in both antibiotic resistance and virulence are smart tools to restore antibiotic treatment efficacy and co-select for avirulent strains (Chan et al. 2018; Gurney et al. 2020). Phages attach to specific bacterial external structures (e.g., flagella, capsules, or efflux pumps) that are involved in important biological processes, such as antibiotic resistance and pathogenicity (Chan et al. 2016; Song et al. 2021; Esteves and Scharf 2022). Modifications in these components make phage infection more difficult and are therefore selected for in bacterial populations exposed to phages. These changes inhibit the bacteria's previous ability to cause disease and to resist antibiotics, thereby restoring their sensitivity to the treatment (Chan et al. 2016; Chiarelli et al. 2020; Gurney et al. 2020). Specifically, bacteria with a downregulated production of efflux pumps would, on the one hand, avoid phage infection. On the other hand, however, they would be more sensitive to antibiotics or toxic heavy metals that are detoxified by these pumps.

A similar mechanism underlies the behavior observed in *Myzus persicae*, an aphid considered a major threat to agriculture (Van Emden and Harrington 2017) and an important living model for the study of insecticide resistance (Bass et al. 2014): mutations in the metabolic activity can lead to the emergence of clones that are more resistant to insecticides due to reduced uptake rates but also more vulnerable to natural enemies (Foster et al. 2007), with nontrivial consequences on their demography (Foster et al. 2011). When exposed to both insecticides and biocontrol (natural enemies or pathogens), insects may face fitness trade-offs that prevent them from maintaining the same level of resistance (Lacey et al. 2015). Therefore, by exerting different selection pressures on a pest, a synergistic use of chemical and biocontrol has the potential to contain resistance development and maintain crop productivity while minimizing the negative environmental impacts by potentially reducing chemical doses (Ons et al. 2020), akin to the phage-antibiotics case.

Since traits that lead to resistance are often also involved in the parasite's ability to exploit and harm the host (Beceiro et al. 2013; Alcalde-Rico et al. 2016; Giraud et al. 2017; Copin et al. 2019), the outcome of a trait-specific treatment may be complicated by the presence of trade-offs between resistance mechanisms and other life history traits of the parasite (Boots and Haraguchi 1999; Boots and Bowers 2004), such as those involving host exploitation and disease-induced mortality (known as the transmission-virulence trade-off) in the case of microparasites (Bull 1994; van den Bosch and Gilligan 2008; Alizon et al. 2009) and those

involving foraging activity and life span in the case of macroparasites (Werner and Anholt 1993; Anholt et al. 2000; Gotthard 2000; Brodin and Johansson 2004; Stoks et al. 2005; Strobbe et al. 2011). Knowledge of novel trait-specific mechanisms is broadening the spectrum of possible selection pressures we can exert on parasites (Allen et al. 2014), and a full exploitation of the potential of such new strategies depends on our understanding of the eco-evolutionary feedbacks between the treatment and the biological system, at various levels of description (Burmeister et al. 2021; Perry 2021).

Accounting for a detailed description of the therapy-parasite interactions have provided insightful information on the in vitro behavior of specific systems (Bull et al. 2014; Mattei et al. 2018; Nichol et al. 2019; Rodriguez-Gonzalez et al. 2020; Aulin et al. 2021). However, their results can be hardly generalizable, and the corresponding population-level information can be tricky to obtain. Here, we are interested in developing a general framework, shared in principle by any control strategy, where (i) treatment efficacy depends on a target trait; (ii) different treatment types correlate differently with the target trait; (iii) target traits are heterogeneously expressed across the parasite population, leading to heterogeneous treatment effects; and (iv) target traits may be related to other parasites' traits through trade-offs.

We tackle this issue by means of a minimal ecological model describing the dynamics of a generic, valuable resource and of a generic parasite population (Lafferty et al. 2015). Following a well-established evolutionary epidemiological approach (Day and Proulx 2004), we model parasites as a trait-structured population, characterized by heterogeneous levels of expression of key traits. We consider a single proxy trait variable accounting for the possible trade-offs between the parasite's level of exploitation and mortality and its resistance to treatment. Crucially and differently from previous work (Frank 1996; Alizon and van Baalen 2005; Porco et al. 2005), we allow treatment efficacy to either correlate or anticorrelate with the proxy trait to reproduce potentially different control strategies as well as combinations of them. We focus our analysis on the implications of trait-dependent treatment from an agricultural perspective, where maximizing resources and reducing treatment use are two major objectives (WHO 2014; Medina-Pastor and Triacchini 2020). Using a simple multicriteria analysis, we show that the ability to tune trait-dependent control can harness parasite heterogeneity to our advantage: in particular, we show the existence of optimal treatment types and the emergence of saturation effects on resource production gains. By focusing on a quantity of general economic interest (healthy resource at equilibrium), our results can be applied to a variety of agricultural practices and are potentially extendable to different scenarios.

Models and Methods

The Model

In the spirit of Lafferty et al. (2015), we start with a minimal ecological model describing the interaction between resource (R) and parasite (P) biomass, potentially representative of both microparasite and macroparasite scenarios. The former scenario neglects the explicit dynamics of within-host abundance (as is commonly done for pathogens; Anderson and May 1979, Keeling and Rohani 2011): R represents the biomass of healthy, susceptible hosts, while P represents the biomass of hosts infected by the pathogen. In the latter scenario (typical of crop-pest and plant-herbivore systems), R represents the resource biomass, and P represents the biomass of the parasite that consumes it. In both scenarios, R is treated as a renewable resource exploited by P. The treatment has the effect of killing the parasite, thus removing P biomass. In what follows, we first present the underlying assumptions of the minimal model, from which we then develop the eco-evolutionary formulation.

Homogeneous RP Formulation with Treatment. Our assumptions are summarized as follows. First, resource biomass is renewed at a constant rate. Second, resource biomass is converted to parasite biomass upon exploitation: in the microparasite scenario, it corresponds to the transmission of the infection from an infected to a susceptible host; in the macroparasite scenario, it corresponds to the consumption of the resource by the consumer. Third, resource and parasite biomass can be removed from the system by various possible mechanisms acting on both (e.g., natural mortality) or either (e.g., disease-induced mortality). Fourth, parasite biomass is eradicated at a rate proportional to treatment application and efficacy: in the microparasite scenario, eradication is intended in the sense of removing the pathogen from the host (Hall et al. 2004; Castle and Gilligan 2012); in the macroparasite scenario, eradication is intended in the sense of killing the parasite (van den Bosch and Gilligan 2008).

Under the above assumptions, the dynamics of R and P biomass is given by the following system of equations:

$$\frac{dR}{dt} = \theta - \delta^R R - \beta RP + \zeta\gamma\phi P, \tag{1a}$$

$$\frac{dP}{dt} = \epsilon\beta RP - (\delta^P + \gamma\phi)P, \tag{1b}$$

where θ is the resource renewal rate; $\delta^{R,P}$ are the mortality rates; β is the exploitation rate; ϵ is the coefficient accounting for biomass conversion; $\gamma\phi$ is the total eradication rate per unit of parasite biomass, where parameter γ is the treatment application rate and ϕ is the treatment efficacy; and ζ is the treated parasite's fate parameter.

In the microparasite scenario, β corresponds to the transmission rate of the infection, and $\epsilon = 1$. The fate of the treated infected host is determined by ζ as follows: for $\zeta = 1$, the treated host is restored to R (i.e., treatment provides recovery without immunity, as may be the case with animal antibiotics; Hethcote 2000; Forster and Gilligan 2007); for $\zeta = 0$, the treated host is removed from the system (recovery with immunity or permanent removal, as is generally the case with plant diseases; Hall et al. 2004). Intermediate values ($0 < \zeta < 1$) can model in-between cases. As will be shown, for our purposes it is not necessary to specify the fate of the treated host, since the results presented here are independent of the value of ζ.

In the macroparasite scenario, β corresponds to the consumption rate of the resource, $0 < \epsilon < 1$ (biomass conversion from resource to consumer) and $\zeta = 0$ (treatment removes consumers from the system).

In the standard ecological formulation of the model, the population is considered to be homogeneous, so that treatment efficacy, exploitation, and mortality rates have constant values across individuals. The behavior of this basic model is well known, and we refer the reader to Korobeinikov and Wake (2002) for details.

Trait-Structured RPx Formulation with Trait-Dependent Treatment. Following previous work (Day and Proulx 2004; Korobeinikov 2018; Day et al. 2020; Sasaki et al. 2022), we elaborate the formulation equivalent to model equations (1) in the case of a parasite heterogeneously expressing a trait. The parameters of the model and their description are summarized in table 1. The following assumptions are introduced. First, the parasite has a continuum of strains, mathematically described by a single continuous proxy variable $x \in \mathcal{T}$, where $\mathcal{T}$ is the trait space. For the sake of simplicity, we will also consider the unit interval $\mathcal{T} = [0, 1]$ as trait space. The generalization to any positive interval $[x_{\min}, x_{\max}]$ is straightforward and can be mapped to the interval [0, 1] by rescaling of the parameters. Heterogeneity is described by the trait distribution $p(x)$, that is, the density of parasites carrying trait x. Second, the trait determines the parasite's levels of resource exploitation, mortality, and treatment efficacy, which are now represented by the functions $\beta(x)$, $\delta^P(x)$, and $\phi(x)$. Third, parasites undergo mutations that induce small changes in their traits and maintain heterogeneity within the population; mutation rates are high compared with the ecological timescale, they are unbiased, and no preferred direction is assumed.

Table 1: Variables and parameters used in the model

	Description
R	Resource biomass
P	Parasite biomass
x	Trait variable
$p(x)$	Parasite trait distribution
$\overline{x}$	Average trait value
μ	Mutations diffusion coefficient
θ	Resource renewal rate
δ^R	Resource mortality rate
γ	Treatment application rate
ζ	Treatment fate parameter
$\delta^P(x)$	Parasite mortality rate
δ_0^P	Parasite baseline natural mortality rate
δ_1^P	Trait-dependent mortality contribution
$\beta(x)$	Parasite exploitation rate
β_0	Baseline exploitation rate
β_1	Trait-dependent exploitation contribution
$\phi(x)$	Trait-dependent treatment efficacy
ϕ_1	Type of treatment ($\lvert\phi_1\rvert$ degree of specialization)

In the heterogeneous formulation, the system is described by the ecological and evolutionary states. The ecological state is given by the amount of R and P biomass. The evolutionary state is given by the trait distribution $p(x)$. Mathematically speaking, $p(x)$ is a probability distribution over which it is possible to compute average quantities with respect to the parasite population. Given the assumptions described above, the dynamics of the heterogeneous system is provided by the following system of equations (details are provided in the supplemental PDF):

$$\frac{dR}{dt} = \theta - \delta^R R - \overline{\beta(t)}RP + \zeta\gamma\overline{\phi(t)}P, \tag{2a}$$

$$\frac{dP}{dt} = \epsilon\overline{\beta(t)}RP - \left[\overline{\delta^P(t)} + \gamma\overline{\phi(t)}\right]P, \tag{2b}$$

$$\frac{dp(x)}{dt} = \mu\frac{\partial^2 p(x)}{\partial x^2} + p(x)[F(x) - \overline{F(t)}], \tag{2c}$$

with

$$F(x) = \epsilon\beta(x)R - \delta^P(x) - \gamma\phi(x). \tag{3}$$

The bar notation indicates the average over the trait distribution; thus, $\overline{\beta(t)}$ is the average exploitation rate of the population:

$$\overline{\beta(t)} = \int_{\mathcal{T}} \beta(x)\, p(x)\, dx. \tag{4}$$

In the equation above, the time dependence is retained in order to recognize that such averages are not fixed but change over time with the time variation of the trait distribution $p(x)$. Equivalent definitions apply to average mortality $\overline{\delta^P(t)}$, the average treatment efficacy $\overline{\phi(t)}$, and the function $\overline{F(t)}$.

Equations (2a) and (2b) describe the population dynamics at the demographic level. They are equivalent to the classical formulation equations (1) upon replacing

the single-strain parameters β, δ^P, and ϕ with their population-average counterparts $\overline{\beta(t)}$, $\overline{\delta^P(t)}$, and $\overline{\phi(t)}$. Equation (2c) instead describes the population dynamics at the evolutionary level, as it governs the changes in the parasite trait distribution due to mutations and competition for limited resource.

Phenotypic mutations are captured by the diffusion operator $\partial^2/\partial x^2$ over the trait space, μ being the diffusion coefficient related to mutations; this choice assumes that mutations induce small perturbations in the quantitative trait, that is, a parasite mutates into a "phenotypically close" variant (possible biases in the direction of mutations may be accounted for by introducing a gradient term in the last equation; Kimura 1965; Chisholm et al. 2016; Lorenzi et al. 2016).

Concomitantly, parasites compete between each other for access to a limited amount of resource (i.e., infection of a limited number of hosts or consumption of a limited resource), according to the trait-dependent function $F(x)$: the exploitation term $\epsilon\beta(x)R$ contributes to increasing the density of trait x, whereas mortality $\delta^P(x)$ and efficacy $\phi(x)$ contribute to decreasing it.

The overall success of parasites with trait x depends on the difference between its value of $F(x)$ and the population average $\overline{F}$, as in a replicator dynamics (Schuster and Sigmund 1983). Thus, $F(x)$ represents the fitness landscape structuring the parasite's competition for exploitation. Unlike purely theoretical work, this fitness landscape is not assumed. Rather, it emerges from the ecological interactions (Day et al. 2020). Note that the evolutionary equation takes the same form regardless of the parasite's nature and of the fate parameter ζ.

The system of equations (2) shows neatly the intertwining of ecological and evolutionary levels of description that is typical of eco-evolutionary dynamics: on the one hand, the demography of the population (given by R and P) depends on the trait distribution $p(x)$ via the average quantities $\overline{\beta(t)}$, $\overline{\delta^P(t)}$, and $\overline{\phi(t)}$; on the other hand, the trait distribution depends on the demography via the ecological interactions (as exploitation depends on R). The solution of the heterogeneous problem (and the methods needed to obtain it) depends on the choice of the trait-dependent functions, which are detailed below.

Trait-Dependent Trade-Offs

We are interested in cases where the proxy trait x provides the parasite with different levels of resource exploitation and, consequently, mortality due to possible life history trade-offs. This trait will also provide a quantitative response to treatment, depending on the type of control strategy employed, so as to model different possible trait-specific treatments and their consequent heterogeneous efficacy. Therefore, in the following we will refer to exploitation, mortality, and efficacy as functions of the proxy trait variable x. Our mathematical choices aim to capture the basic biological features of the trade-offs of interest while maintaining mathematical tractability. Relaxation of such choices does not alter the qualitative features of our model (details are provided in the supplemental PDF). References to the examples presented in the introduction should be taken as qualitative connections underpinning our approach rather than exact, detailed descriptions of the resistance, exploitation, and mortality mechanisms at play.

Exploitation. We assume exploitation rate β to be linearly affected by the trait variable x; that is,

$$\beta(x) = \beta_0 + \beta_1 x, \tag{5}$$

where β_0 is the baseline rate and β_1 the trait-dependent contribution. We recall that in the microparasite scenario equation (5) corresponds to the transmission rate of the infection, and in the macroparasite scenario it corresponds to the consumption rate.

Mortality. In the microparasite scenario, increased exploitation (i.e., transmission rate) is often associated with increased harm to the infected host (i.e., the transmission-virulence trade-off; Montarry et al. 2006; Sacristán and García-Arenal 2008; Laine and Barrès 2013; Zhan et al. 2015; Nelson and May 2020); in the macroparasite scenario, increased exploitation (i.e., consumption rate) is often associated with a reduced parasite life span due to, for example, increased respiration or risk exposure (Werner and Anholt 1993; Anholt et al. 2000; Gotthard 2000; Brodin and Johansson 2004; Stoks et al. 2005; Strobbe et al. 2011). In both scenarios, the respective trade-offs lead to an increase in parasite mortality. Accordingly, we assume that parasite mortality δ^P can be linearly dependent on trait x:

$$\delta^P(x) = \delta_0^P + \delta_1^P x, \tag{6}$$

where the parameter δ_0^P is the baseline natural mortality and δ_1^P is the trait-dependent contribution (Day and Proulx 2004; Porco et al. 2005; Bolzoni and De Leo 2013).

For values of both δ_1^P and $\beta_1 > 0$, parasites with higher exploitation will also have higher mortality, consistent with the trade-off hypothesis described above.

Treatment Efficacy. We assume that efficacy $\phi(x)$ is maximal for one of the extreme values of the trait ($x = 0$ and $x = 1$). Consistent with Porco et al. (2005), we choose a linear functional dependence:

$$\phi(x) = C_{\phi_1} + \phi_1 x, \tag{7}$$

where the parameter ϕ_1 represents the degree of correlation between the treatment and the trait (as explained in the next subsection) and C_{ϕ_1} is a normalization factor. A

graphical summary of the treatment spectrum is shown in figure 1*B* (note that the bound $|\phi_1| < 2$ ensures a positive $\phi(x)$). The linear assumption is made for the sake of mathematical tractability, although nonlinear saturating choices are considered more realistic (Alizon 2020). The effects of nonlinearities can be explored semianalytically, but they do not affect the quality of the results presented herein (details are provided in the supplemental PDF).

Combination of equations (5), (6), and (7) captures the possible trade-offs occurring between trait-dependent treatment efficacy and the parasite's exploitation levels. Ultimately, the eco-evolutionary dynamics of the system depends on the values of the parameters of the functions described above and thus on how a control strategy interacts with the proxy trait value x.

Modeling Treatment Spectrum

We assume that the environmental and economic costs of the use of treatment are proportional to its application rate γ. We also assume that trait x determines the level of expression of a target trait, such as efflux pump expression, metabolic activity, or proton motive force. The type of treatment then depends on how it correlates with the target trait, which is specified by the slope parameter ϕ_1.

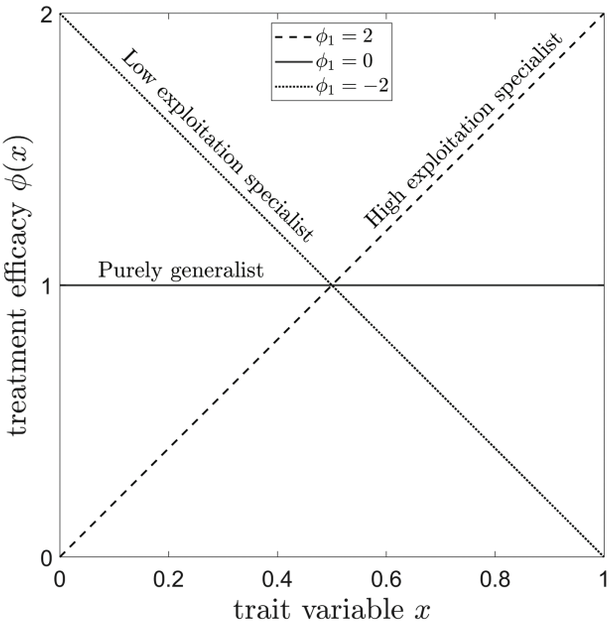

Figure 1: Spectrum of treatments with trait-dependent efficacy. The type of treatment is determined by the sign and the magnitude of the parameter $\phi_1 \in [-2, 2]$: positive ϕ_1 models types with maximal effect on strains with higher exploitation levels ($x = 1$), and negative ϕ_1 models types with maximal effect on strains with lower exploitation levels ($x = 0$). Large $|\phi_1|$ are specialized in targeting extreme values of the trait, and small $|\phi_1|$ are generalist types with more uniform action.

For instance, efflux pumps provide bacteria with resistance to chemical compounds but make them vulnerable to attack by certain phages. Therefore, a standard antibiotic or pesticide treatment is more efficient on strains with lower levels of efflux pump expression (small x), and it is represented by a negative ϕ_1; instead, phage therapy benefits from higher levels of efflux pump expression (large x), and it is represented by a positive ϕ_1.

Metabolic activity provides aphids an increased ability to consume and reproduce, but it also makes them also more sensitive to pesticides, as they will tend to take up more toxic compounds. Therefore, the pesticide is more efficient on fast-exploiting strains (large x) and less efficient on slow-exploiting strains (small x); its slope ϕ_1 is then positive. At the same time, reduced metabolic activity makes the aphids more vulnerable to natural enemies, so that predator-based biocontrol will have a negative ϕ_1.

Proton motive force reduces the import of aminoglycosides but also the export of β-lactams. Therefore, aminoglycoside is more efficient against strains expressing less proton motive force (small x) and less efficient against strains with more proton motive force (large x); it is thus represented by a negative ϕ_1. However, β-lactam has the opposite effect, so it is represented by a positive ϕ_1.

In any case, maximal efficacy is obtained at the extremes of the trait space (either $x = 0$ or $x = 1$), so it is assumed that the correlation of efficacy with traits is unimodal. In the absence of more precise data, we consider this assumption to be a reasonable starting point and leave other possible cases for discussion. The normalization factor $C_{\phi_1} = 1 - \phi_1/2$ ensures that $\int_T \phi(x)dx$ is always normalized to 1, for any value of ϕ_1. In addition to removing an arbitrary degree of freedom, this condition also imposes a plausible evolutionary constraint consistent with the notions of costs of resistance and of collateral sensitivity: resistance with respect to a particular treatment is paid for by high sensitivity with respect to others, as has been observed in the examples illustrated above.

Recognizing that a treatment may be either positively or negatively correlated with the proxy trait variable, we assume the existence of a continuous spectrum from which it is, in principle, possible to choose. This continuous spectrum mimics the possibility of synergistically combining different types of treatments, as has been documented for phages and antibiotics (Gu Liu et al. 2020; Kebriaei et al. 2022), antibiotics and antivirulents (Rezzoagli et al. 2020), fungicide mixtures (van den Bosch et al. 2014), antibiotic mixtures (Cokol et al. 2011; Nichol et al. 2019), fungicide biocontrol (Lima et al. 2006), and pesticide biocontrol (Foster et al. 2007). Crucially, we assume that the overall efficacy

is the result of the sum of the single different treatment types. Therefore, any slope can be obtained by adjusting the relative proportions of antibiotic and phage therapy. Although we expect a full spectrum to be practically unavailable, it allows us to fully explore the eco-evolutionary behavior of the system. Henceforth, the term "specialist" will refer to treatments with a large degree of correlation (large $|\phi_1|$), and the term "generalist" will refer to treatments with a small degree of correlation (small $|\phi_1|$). A control strategy is thus characterized by one value of application rate γ and one value of treatment type ϕ_1.

Agent-Based Numerical Simulations

We compared the deterministic dynamics presented in our article with numerical simulations of the equivalent agent-based dynamics. The Python code is available from Zenodo (https://zenodo.org/record/7874696#.ZFu4AnZBybh; Miele et al. 2023). The agent-based dynamics simulates the stochastic events of renewal, mortality, exploitation, treatment, and mutation, each occurring at a rate consistent with the deterministic equations (2). The deterministic theory is expected to be consistent with our agent-based simulations as long as large populations are involved. Our aim is to provide a numerical validation of the existence and stability of the endemic equilibrium solution predicted by the theory. The analysis of finite size effects on the system is beyond the scope of this article, although it is straightforward to perform once the agent-based codes are set up (Ardaševa et al. 2020). Details of the numerical simulations can be found in the supplemental PDF.

Results

Equilibrium Trait Distribution and Evolutionary States

The state of the parasite population at equilibrium is described by the steady-state trait distribution $p(x)$, the solution of

$$\mu \frac{\partial^2 \widehat{p(x)}}{\partial x^2} + \widehat{p(x)}[F(x) - \overline{F}] = 0, \tag{8}$$

where the average quantities $\overline{\beta}$, $\overline{\delta^P}$, and $\overline{\phi}$, appearing in $\overline{F}$, are not known a priori, as they depend on the solution $p(x)$ itself. Note that their time dependence has been dropped, since they reach a constant value at equilibrium. The equation given above has a trivial solution $\widehat{p_0(x)} = 0$, corresponding to the parasite-free equilibrium, and a nontrivial solution describing the endemic equilibrium, where resource and parasites coexist (mathematical details are provided in the supplemental PDF).

The coexistence equilibrium exists (and is stable) as long as the following condition is satisfied:

$$R_0 = \frac{\theta}{\delta^R} \frac{\epsilon \overline{\beta}}{\overline{\delta^P} + \gamma \overline{\phi}} \geq 1, \tag{9}$$

where R_0 is the expected offspring produced by a parasite encountering an unexploited resource, per unit of biomass (also known as the basic reproduction number), for the heterogeneous system. Contrary to the classical formulation, the condition described above cannot be calculated directly in terms of the ecological parameters, since it depends on average quantities that are not known a priori. Therefore, one must first solve equation (8) for a given set of parameters, then calculate the average quantities and check with condition equation (9) the existence of the endemic equilibrium. In the supplemental PDF, we show that the behavior of the solution to equation (8), with linear trait-dependent functions, is entirely determined by the following compound parameter Ω:

$$\Omega = \beta_1 \delta_0^P - \beta_0 \delta_1^P + \gamma(\beta_1 - \beta_1 \phi_1/2 - \beta_0 \phi_1). \tag{10}$$

In particular, if $\Omega < 0$, the solution is monotonically decreasing and the trait distribution is mostly distributed close to the trait $x = 0$. We will refer to this as the "low-exploitation" state because the corresponding trait has a minimum value for $x = 0$. On the other hand, if $\Omega > 0$, the solution is monotonically increasing and the trait distribution is mostly distributed close to the trait $x = 1$. Likewise, we will refer to this as the "high-exploitation" state.

Below we characterize the phase diagram corresponding to a set of parameters, both in the presence and in the absence of treatment. In this case, the proxy trait variable x simultaneously determines the levels of transmission and mortality of the parasite as well as the efficacy of the treatment. In the absence of treatment (i.e., $\gamma = 0$), the parasite population can be found in either the high- or low-exploitation state, depending on the value of the ecological parameters. With reference to figure 2*A*, low states will be favored for large baseline exploitation β_0 and trait-dependent mortality contribution δ_1^P; instead, high states will be favored for large trait-dependent exploitation β_1 and baseline mortality δ_0^P.

The introduction of treatment (i.e., $\gamma \neq 0$) can lead to a change in state, depending on the control strategy (ϕ_1, γ) employed. In figure 2*B*, we show how a system initially in the low state (parameters corresponding to the red point in fig. 2*A*) adapts after treatment application, as a function of the control parameters γ and ϕ_1. At low doses (i.e., low γ), the parasite population will remain in the low state, regardless of the type employed. However, increasing the application rate will eventually bring the system to the high state if negative ϕ_1 or generalist types are employed. If the system is initially in the high state in the absence of treatment (fig. 2*C*; blue point of fig. 2*A*), the complementary behavior is observed.

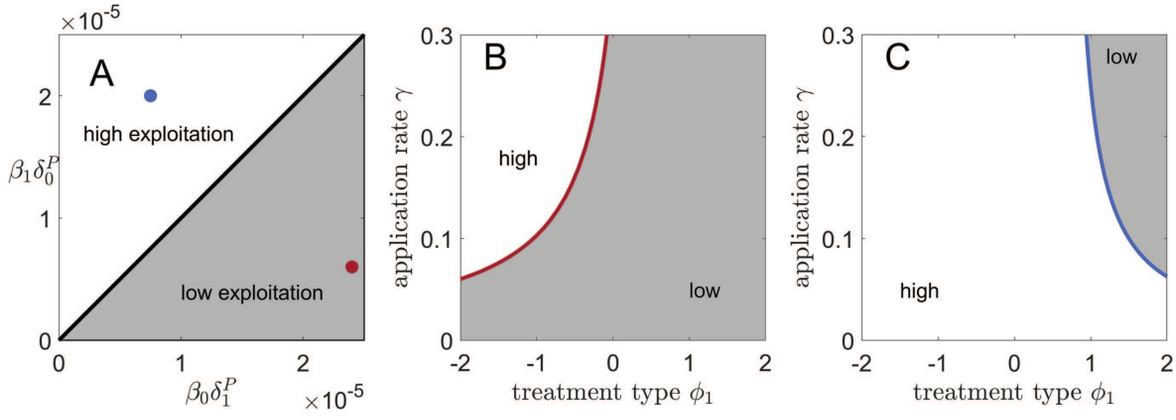

Figure 2: Trait distribution states. *A*, State diagram of the trait distribution in the absence of treatment. The parasite population can adapt toward either low-exploitation (gray regions) or high-exploitation (white regions) states. *B*, A system initially in the low state (red point in *A*) can switch toward the high state under a range of control strategies. The red curve separates the two regions of the control parameters. *C*, Likewise, a system initially in the high state (blue point in *A*) can switch toward the low state under a range of control strategies. The blue curve separates the two regions of the control parameters. Parameters: for the red point, $\beta_0 = 0.0001$, $\beta_1 = \beta_0/2$, $\delta_0^P = 0.12$, $\delta_1^P = 0.24$; for the blue point, $\beta_0 = \beta_1 = 0.0001$, $\delta_0^P = 0.2$, $\delta_1^P = 0.075$.

In addition to affecting the evolutionary state of the system at endemic equilibrium, the control strategy also affects the amount of equilibrium resource. The adaptation toward the two possible states is shown in figure 3, where we plot the trajectories of the simulated agent-based dynamics (solid lines), differing for the treatment type employed. The other parameters (indicated in the figure caption) and initial conditions are identical. For $\phi_1 = 2$ the system adapts toward the low state, and for $\phi_1 = -2$ it adapts toward the high state. Consequently, the resource reached at equilibrium is

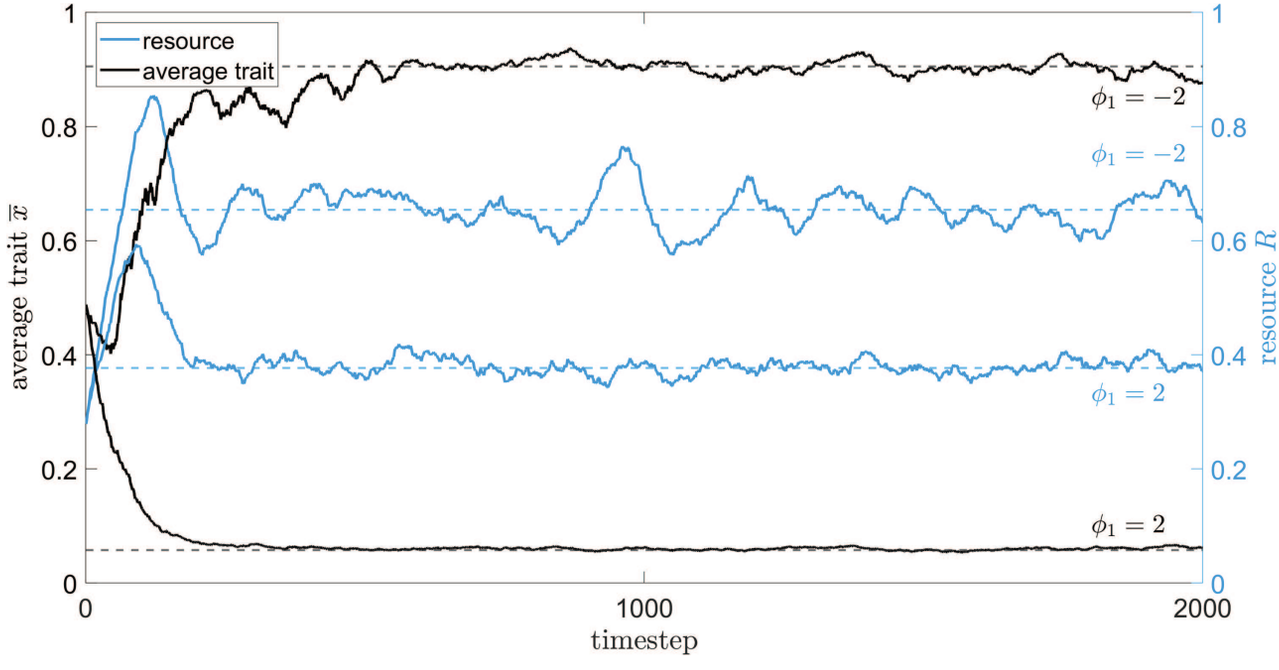

Figure 3: Simulated temporal trajectories. Solid lines: temporal trajectories of the resource R (rescaled with respect to R_0) and of the average trait $\bar{x}$, obtained from agent-based numerical simulations of the dynamics. Dashed lines: analytical equilibrium values predicted by the deterministic theory. The system is initialized with identical initial conditions and the same application rate $\gamma = 0.1$ but a different treatment type ϕ_1. For $\phi_1 = \pm 2$, resource and parasite average trait attain different equilibrium values. Other parameters: $\theta = 200$, $\delta^R = 0.04$, $\beta_0 = 0.0001$, $\beta_1 = \beta_0/2$, $\delta_0^P = 0.12$, $\delta_1^P = 2\delta_0^P$, $\mu = 7 \times 10^{-5}$.

different in the two cases. The figure also shows the agreement between the analytical predictions for the equilibrium values (dashed lines) and the agent-based trajectories (solid lines), which holds for all sets of parameters considered in our analysis.

Equilibrium Resource and Treatment Effects

In the following, we will focus on the equilibrium resource R, which can be considered as the amount of harvest with economic value (Cunniffe et al. 2015; Vyska et al. 2016). The population equilibria are obtained by setting equations (2) to zero, and they are equivalent to the classical formulation. If $R_0 < 1$, we have a trivial parasite-free equilibrium:

$$\left(\widehat{R}_0 = \frac{\theta}{\delta^R}; \widehat{P}_0 = 0\right), \tag{11}$$

corresponding to the extinction of the parasite. If $R_0 \geq 1$, we have the following stable endemic equilibrium:

$$\left(\widehat{R} = \frac{\overline{\delta^P} + \gamma\overline{\phi}}{\epsilon\overline{\beta}}; \widehat{P} = \frac{\epsilon\overline{\beta}\theta - \delta^R(\overline{\delta^P} + \gamma\overline{\phi})}{\overline{\beta}[\overline{\delta^P} + \gamma\overline{\phi}(1-\zeta)]}\right). \tag{12}$$

Note that the equilibrium averages are function of the control strategy (ϕ_1, γ), since the equilibrium trait distribution $p(x)$ depends on such parameters. Therefore, equation (12) provides all the information about the complex relationship between resource production and control strategy, and it allows the systematic exploration of the whole parameter space. Note that the value of resource at the endemic equilibrium R is independent of ζ. Therefore, a control strategy with such a quantity as the objective will have the same outcome regardless of the fate of the treated parasite. In the following, we will focus on a particular set of parameters as an example of the relevant behavior of the system.

In figure 4, we plot the equilibrium resource R (rescaled with respect to the parasite-free resource R_0) as a function of application rate γ and compare the effect of five different types of treatment: $\phi_1 = -2$, -1, 0, 1, and 2. We present two sets of parameters corresponding to the two opposite states of the parasite trait distribution in the absence of treatment: the left panel corresponds to the red point in figure 2*A*, which is a low-exploitation state; the right panel corresponds to the blue point in figure 2*A*, which is a high-exploitation state. Note that employing a treatment type that is inconsistent with the state of the trait distribution in the absence of control (e.g., $\phi_1 = 2$ for the left panel, $\phi_1 = -2$ for the right panel) leads to a small increase in resource as the dose increases (green and blue curves, respectively). Instead, employing a type extremely specialized in the trait that dominates in the absence of control ($\phi_1 = -2$ for the left panel, $\phi_1 = 2$ for the right panel) leads to a more significant increase in resource, at least for low application rates (blue and green curves, respectively). However, as increasing the rate of application tends to push the system toward the opposite state, extremely specialized treatments can quickly become less effective, and the resource gain will eventually saturate. At this point, switching to a more moderate type (smaller ϕ_1) rather than further increasing the application rate γ will provide more resource gain. Depending on the value of the renewal rate θ, the system may eventually reach the parasite-free equilibrium (where $\widehat{R} \equiv \widehat{R}_0$). Overall, when comparing the two panels, we find that the outcome of the control depends on the state of the parasite population in the absence of treatment, so that very efficient treatments in one case may be very inefficient in the other. We also find that an increase in γ, regardless of the choice, always corresponds to an increase in the resource. Therefore, maximizing the resource and minimizing the treatment application are conflicting objectives. Nevertheless, it is possible to identify efficient strategies (ϕ_1, γ), as explained below.

Pareto-Efficient Strategies

Figure 4 shows that resource maximization and treatment application minimization are conflicting objectives. In the presence of conflicting objectives, multicriteria analysis highlights the best compromises in the form of Pareto-efficient solutions (Kennedy et al. 2008). Among all of the possible choices of our control strategy (ϕ_1, γ), the Pareto-efficient solutions are those for which it is not possible to improve one objective without worsening the other. As such, they provide the decision maker with a smaller set of privileged alternatives to choose from, depending on the different management scenarios and on the decision maker's priorities.

The resulting Pareto-efficient solutions to our control strategy are identified by the solid curves in figure 4: choosing a control strategy (ϕ_1, γ) different from the Pareto-efficient ones will inevitably worsen the outcome (dashed curves) either by reducing the amount of resource or by increasing the costs associated with the treatment application.

We note that when moving along the same type ϕ_1, the resource shows a decrease in the incremental gain for the following threshold application rate:

$$\gamma^{\text{th}}(\phi_1) = \frac{2(\beta_1\delta_0^P - \beta_0\delta_1^P)}{(2\beta_0 + \beta_1)\phi_1 - 2\beta_1}. \tag{13}$$

In the presence of a constraint on the application rate, the problem collapses to a unique objective function, which is optimized by (mathematical details in the supplemental PDF)

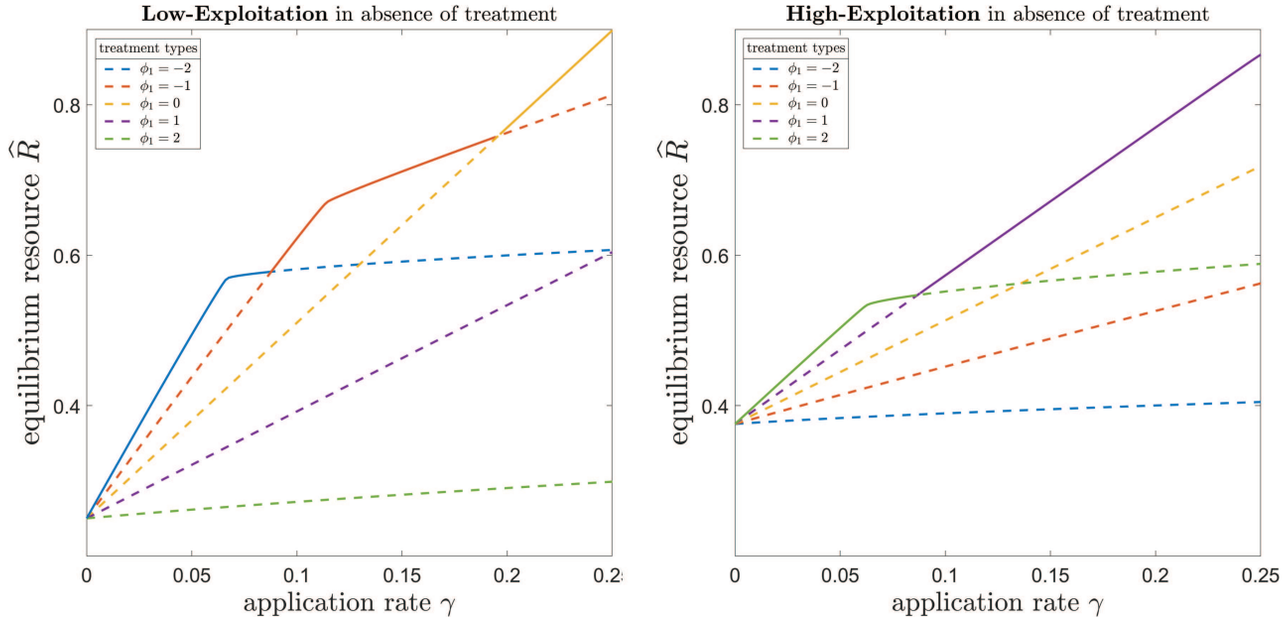

Figure 4: Equilibrium resource as function of control strategy. Shown is the resource at equilibrium R obtained using five different treatment types, as a function of application rate γ (the y-axis is normalized with respect to the disease-free resource R_0). *Left*, in the absence of treatment, the system is in the low-exploitation state; parameters correspond to the red point of figure 2. *Right*, in the absence of treatment, the system is in the high-exploitation state; parameters correspond to the blue point of figure 2. Very specialized types ($\phi_1 = \pm 2$) are efficient for low γ, but their correspondent gain in resource saturates as the application rate is increased. Therefore, if the application rate can be increased, more generalist treatment should be privileged. The Pareto-efficient strategies of the control strategy are highlighted with solid curves. Other parameters: $\mu = 7 \times 10^{-5}$, $\theta = 150$, $\delta^R = 0.04$.

$$\phi_1^{\text{opt}}(\gamma) = \frac{2}{2\beta_0 + \beta_1}\left(\frac{\beta_1\delta_0^P - \beta_0\delta_1^P}{\gamma} + \beta_1\right). \qquad (14)$$

With respect to figure 2, the equation given above corresponds to the curves separating the two states in the (ϕ_1, γ) phase diagrams, for which $\Omega = 0$. The effect of each parameter on $\phi_1^{\text{opt}}(\gamma)$ is summarized in table 2. In particular, we note that the optimal degree of specialization is a decreasing function of application rate γ, so that extremely specialized treatments types will perform better at low γ; the optimal choice is independent of biomass conversion ϵ; and exploitation and mortality rates (both baseline and trait-dependent contributions) play a nontrivial role in shaping the optimal choice.

Overall, equations (13) and (14) provide qualitative insight into the role played by each ecological interaction in shaping the control strategy behavior.

Discussion

We have developed a mathematical model to explore the implications of possible correlations between treatment efficacy and key traits of the parasite. We have considered a general parasite that may express continuous levels of exploitation and mortality (eqq. [5], [6]) and a treatment that exerts an eradicant action, which may be either positively or negatively correlated with the levels given above (eq. [7]; fig. 1), depending on the type of treatment. As a result of eco-evolutionary feedback, the parasite population can adapt toward evolutionary states dominated by either high or low exploitation levels (fig. 2), and the final resource will depend on the control strategy employed (fig. 4). The transition between these two possible states triggers several implications, depending on the management scenarios, which we discuss below.

Scenario 1: both the application rate and treatment type are freely tunable. In this case, the efficient strategies are represented by a Pareto front (solid lines in fig. 4). The Pareto front does not identify a single best strategy. Rather, it highlights a collection of best compromises between resource production and treatment use: whether to favor economic, environmental, or ethical objectives will therefore depend on the priorities of the decision maker, as well as on how the resource and the application rate will map into a real cost benefit.

Scenario 2: the type of treatment may be constrained by the unavailability of alternatives or the inability to play with synergistic effects. In this case, there will be a threshold γ^{th}, above which the decision maker should begin to question the benefit of further increasing the application rate.

Table 2: Effect of the parameters on the Pareto-efficient strategies

Parameter	Effect on $\phi_1^{\text{opt}}(\gamma)$	Effect on $\gamma^{\text{th}}(\phi_1)$
γ	$\uparrow$ if $(\beta_0\delta_1^P - \beta_1\delta_0^P) < 0$ and $\downarrow$ otherwise	...
$\lvert\phi_1\rvert$	...	$\downarrow$ always
β_0	$\uparrow$ if $(\delta_0^P + \delta_1^P/2 - \gamma) > 0$ and $\downarrow$ otherwise	$\downarrow$ always
β_1	$\uparrow$ if $(\delta_0^P + \delta_1^P/2 - \gamma) < 0$ and $\downarrow$ otherwise	$\downarrow$ always
δ_0^P	$\uparrow$ always	$\uparrow$ always
δ_1^P	$\downarrow$ always	$\downarrow$ always

Note: The symbol $\uparrow$ ($\downarrow$) indicates that an increase in the parameter in question leads to an increase (decrease) of $\phi_1^{\text{opt}}(\gamma)$ and $\gamma^{\text{th}}(\phi_1)$.

The economic impact of these saturation effects can be further assessed by including such information in economic evaluations of agricultural systems (Paveley et al. 2001; Ney et al. 2013; Day et al. 2021). Note that these saturation effects differ from those typically reported in the literature with treatment dose-response curves (Elderfield et al. 2018), which are accounted for by using nonlinear, saturating functions. Here, saturation is due to a transition between opposite evolutionary states. This kind of saturation is then dynamic, and it is inherent to the eco-evolutionary nature of the system.

Scenario 3: the application rate may be constrained by limits on the use of antibiotics for safety reasons or by limits on the spread of pesticides/copper/fungicides for legislative agricultural constraints. In this case, there will be a unique optimal type ϕ_1^{opt}. As a general rule, very specialized treatment types should be employed at low application rates; instead, generalist types, with a more uniform action over the trait space, are likely to perform better at high application rates. This value represents the optimal choice from an ideal continuous spectrum of possibilities. We do not expect this spectrum to be fully available or even possible to design in practice. Nevertheless, it should provide qualitative guidance to the decision maker when calibrating synergistic treatments.

These scenarios assume that the control parameters ϕ_1 and γ are independent, which may not always be the case. However, a possible relation between application rate and treatment could be considered if the function $\gamma(\phi_1)$ is known. Similarly, treatment application may be related to aspects of the host-parasite system (e.g., virulence or severity of the symptoms; Porco et al. 2005). In such cases, it may be possible to derive optimal treatment conditions in terms of the epidemiological parameters of the parasite, provided that the corresponding functions are known.

Overall, our results can contribute to the ubiquitous call to reduce the use of chemicals in public health (WHO 2014) and agriculture (Medina-Pastor and Triacchini 2020). Specifically, they point toward many of the European Union's principles (P) for sustainable farm management (Barzman et al. 2015): valuable synergistic use of alternative control methods (P4), minimizing environmental impact (P5), reducing the use of chemicals (P6), and antiresistance strategies (P7). A concrete and urgent issue is the widespread use of copper in agriculture to combat plant diseases (Nunes et al. 2016). Because of its questionable efficacy and toxic side effects, there is an urgent call for its reduction (Tamm et al. 2018). In bacteria, resistance to heavy metals such as copper is mediated by efflux pumps, which are also involved in virulence to plants (Ryan et al. 2007; Martinez et al. 2009). Therefore, our theoretical framework could be used to support experimental studies of phage-copper synergy, which remain to be tested.

The assumption of a broad spectrum of treatment effects was motivated by the growing interest in developing therapies targeting specific traits and the possibility of combining them synergistically with traditional synthetic treatments (Lima et al. 2006; Allen et al. 2014; Baym et al. 2016). So far, we have referred to collateral sensitivity, phage therapy, and biocontrol as examples of control strategies that interfere with heterogeneous traits involved in both resistance and resource exploitation. We argue that the phenomenon may be of interest to other treatments based on heterogeneity and evolutionary constraints, such as antibiofilm, photodynamic activation, and more, on phage therapy.

Antibiofilm and photodynamic activation rely on a planktonic-versus-sessile evolutionary trade-off (Almeida et al. 2014; Tits et al. 2020; Feng et al. 2021): some bacteria can either live and move individually (planktonic phase) or can aggregate together into immobile structures called biofilms (sessile phase). Targeting such structures is a desirable strategy because they are involved in virulence and resistance to treatment. However, the efficacy of an antibiofilm treatment would depend on the trait composition of the target bacterial population, which in turn depends on the trade-off between the two phases, similar to the phenomenon considered in this work.

A promising application of phage therapy is the use of phages that have bacterial capsules as receptors. Capsules

are external polysaccharide layers that protect bacteria and facilitate attachment to host tissue. Capsules are therefore involved in host colonization and in evasion of the immune response or treatment. Phage selection for reduced capsule production will impose trade-offs between virulence and antibiotic sensitivity (Chiarelli et al. 2020; Song et al. 2021).

A proper experimental investigation and measurement of specific trait-dependent effects would likely require two stages. The first would be a single-cell stage to detect heterogeneity in the level of expression of the trait of interest and to measure the resulting trait-dependent interactions with the different treatments (Fernandes et al. 2011); this task could be performed using in vitro setups, such as microscopy, flow cytometry, or RNA sequencing (Avraham et al. 2015; Mohiuddin et al. 2020). The second would be a population stage where the overall effects on the demography and on the trait distributions can be monitored and measured; this task could be performed in controlled in vivo environments, such as bioreactors (Levin and Udekwu 2010), greenhouses, field plots, and animal facilities (Band et al. 2016).

Our analysis has assumed a linear, monotonic, and unimodal dose-response curve for treatment efficacy so as to keep the model as simple as possible and to favor mathematical tractability. In the supplement PDF, we show that the addition of nonlinearities does not affect the qualitative behavior of the system as long as an evolutionary constraint is considered. Therefore, we conjecture that the emergence of optimal and threshold behaviors are inherent to the system and that they are due to evolutionary constraints, rather than to its exact functional form. From a theoretical perspective, it would be interesting to prove this conjecture formally, for any kind of evolutionary constraint imposed on the treatment.

Instead, we expect that breaking the unimodal assumption will have nontrivial implications. On the one hand, a bimodal efficacy function would likely trigger multiple peaks in the trait distributions, therefore leading to possible branching phenomena where the parasite population splits into two separate subclasses of, for example, mid-low and mid-high levels of exploitation; however, we are currently unaware of any evidence for bimodal treatment efficacy, and it would need to be motivated by (at least) phenomenological arguments. On the other hand, it is reasonable to imagine a treatment that would have maximal efficacy at an intermediate value of the proxy trait (rather than at the extremes), which would likely lead to nonmonotonous trait distributions; accordingly, the variance of this putative bell-shaped efficacy could function as a tunable control parameter, governing possible intermediate scenarios between the homogeneous (rather flat, large variance) and the heterogeneous (rather peaked, small variance) extremes.

Although nonlinear, concave-down functions are typically considered to relate exploitation and mortality, a simpler linear choice has allowed us to take full advantage of the mathematical analysis while preserving the possibility to model exploitation-mortality trade-offs; it also provides the baseline results against which to compare nonlinear functions, thus disentangling the role of nonlinearities from the role of the trade-off alone. The relaxation to nonlinear functions is discussed in the supplement PDF, where it is again shown that the qualitative behavior of the linear case is preserved.

Although our analytical derivation of the optimal treatment type relies on many simplifying assumptions, our work highlights the qualitative role of the various epidemiological interactions, and it provides a starting point for introducing further elements of complexity. To conclude our discussion, we highlight some potentially interesting issues.

Although multidimensional trait spaces are rarely considered, the simultaneous presence of multiple traits encoding different features of the parasite would improve the realism of the model. In particular, it would be interesting to explore the case where the treatment correlates with a subset of them, in order to mimic intervention policies with imperfect coverage (Walter and Lion 2021). For instance, one could consider a pathogen endowed with a trait defining its transmission capacity and a trait defining its disease-induced mortality; then one could imagine the existence of an intervention affecting the transmission trait (e.g., protectant effects of a pesticide, quarantine policy, vaccination campaigns) and an intervention affecting the mortality trait. Performing a similar analysis, one might be able to compute the optimal combination of the two actions and relate it to the geometry of the trait space (Miele et al. 2021), as well as to the possible evolutionary and economic constraints.

Our minimal model used simple demography for both resource and parasite dynamics. The introduction of more complex demographic functions (Cunniffe and Gilligan 2010) could lead to oscillating regimes around the endemic equilibrium. Such a maintained out-of-equilibrium demography results in a time-varying fitness landscape that could trigger out-of-equilibrium evolutionary responses, characterized by the alternation of low- and high-exploitation regimes of the trait distribution.

The expanding knowledge of the ecological, evolutionary, and molecular interactions between parasites and treatments, coupled with the theoretical feedback, should continue to provide opportunities to effectively address the challenge of disease management. Combining the practical development of trait-specific treatments with our theoretical methods of investigation (Saubin et al. 2023) may allow us to exploit heterogeneity of parasite populations—almost always seen as a key difficulty by allowing the evolution of resistance to human intervention—to

our advantage. Ultimately, evolutionary epidemiology is an instantiation of a more general theory of evolutionary ecology (Lion 2018). As such, the potential of the approach presented here can be exploited to investigate trait-dependent intervention in other domains, such as public health (Stearns 2012) and cancer dynamics (Gatenby et al. 2009).

Acknowledgments

L.M. is grateful to Jacopo Lupi and Lorenzo Tinacci for thoughtful conversations. L.M. and D.B. thank Bertrand Gauffrè and Nick Taylor for preliminary discussions. This work was supported by the Natural Environment Research Council (NERC) Doctoral Training Partnership (DTP; studentship NE/L002574/1) and by the Engineering and Physical Sciences Research Council (EPSRC).

Statement of Authorship

Conceptualization: L.M., R.M.L.E., D.B. Funding acquisition: R.M.L.E. Methods development: L.M. Model analysis: L.M. Coding simulation: L.M. Supervision: R.M.L.E., D.B. Writing—original draft: L.M. Writing—review and editing: L.M., R.M.L.E., N.J.C., C.T.-B., D.B.

Data and Code Availability

Code is available from Zenodo (https://zenodo.org/record/7874696#.ZFu4AnZBybh; Miele et al. 2023).

Literature Cited

Alcalde-Rico, M., S. Hernando-Amado, P. Blanco, and J. L. Martínez. 2016. Multidrug efflux pumps at the crossroad between antibiotic resistance and bacterial virulence. Frontiers in Microbiology 7:1483.

Alekshun, M. N., and S. B. Levy. 2007. Molecular mechanisms of antibacterial multidrug resistance. Cell 128:1037–1050.

Alizon, S. 2020. Treating symptomatic infections and the co-evolution of virulence and drug resistance. bioRxiv, https://doi.org/10.1101/2020.02.29.970905.

Alizon, S., A. Hurford, N. Mideo, and M. Van Baalen. 2009. Virulence evolution and the trade-off hypothesis: history, current state of affairs and the future. Journal of Evolutionary Biology 22:245–259.

Alizon, S., and M. van Baalen. 2005. Emergence of a convex trade-off between transmission and virulence. American Naturalist 165:E155–E167.

Allen, R. C., R. Popat, S. P. Diggle, and S. P. Brown. 2014. Targeting virulence: can we make evolution-proof drugs? Nature Reviews Microbiology 12:300–308.

Almeida, J., J. P. Tomé, M. G. Neves, A. C. Tomé, J. A. Cavaleiro, Â. Cunha, L. Costa, M. A. Faustino, and A. Almeida. 2014. Photodynamic inactivation of multidrug-resistant bacteria in hospital wastewaters: influence of residual antibiotics. Photochemical and Photobiological Sciences 13:626–633.

Anderson, R. M., and R. M. May. 1979. Population biology of infectious diseases: part I. Nature 280:361–367.

Andersson, D. I., and D. Hughes. 2010. Antibiotic resistance and its cost: is it possible to reverse resistance? Nature Reviews Microbiology 8:260–271.

Anholt, B. R., E. Werner, and D. K. Skelly. 2000. Effect of food and predators on the activity of four larval ranid frogs. Ecology 81:3509–3521.

Ardaševa, A., A. R. Anderson, R. A. Gatenby, H. M. Byrne, P. K. Maini, and T. Lorenzi. 2020. Comparative study between discrete and continuum models for the evolution of competing phenotype-structured cell populations in dynamical environments. Physical Review E 102:042404.

Aulin, L., A. Liakopoulos, P. H. van der Graaf, D. E. Rozen, and J. van Hasselt. 2021. Design principles of collateral sensitivity-based dosing strategies. Nature Communications 12:5691.

Avraham, R., N. Haseley, D. Brown, C. Penaranda, H. B. Jijon, J. J. Trombetta, R. Satija, et al. 2015. Pathogen cell-to-cell variability drives heterogeneity in host immune responses. Cell 162:1309–1321.

Band, V. I., E. K. Crispell, B. A. Napier, C. M. Herrera, G. K. Tharp, K. Vavikolanu, J. Pohl, et al. 2016. Antibiotic failure mediated by a resistant subpopulation in *Enterobacter cloacae*. Nature Microbiology 1:16053.

Barbosa, C., R. Römhild, P. Rosenstiel, and H. Schulenburg. 2019. Evolutionary stability of collateral sensitivity to antibiotics in the model pathogen *Pseudomonas aeruginosa*. eLife 8:e51481.

Bargués-Ribera, M., and C. S. Gokhale. 2020. Eco-evolutionary agriculture: host-pathogen dynamics in crop rotations. PLoS Computational Biology 16:e1007546.

Barzman, M., P. Bàrberi, A. N. E. Birch, P. Boonekamp, S. Dachbrodt-Saaydeh, B. Graf, B. Hommel, et al. 2015. Eight principles of integrated pest management. Agronomy for Sustainable Development 35:1199–1215.

Bass, C., A. M. Puinean, C. T. Zimmer, I. Denholm, L. M. Field, S. P. Foster, O. Gutbrod, R. Nauen, R. Slater, and M. S. Williamson. 2014. The evolution of insecticide resistance in the peach potato aphid, *Myzus persicae*. Insect Biochemistry and Molecular Biology 51:41–51.

Baym, M., L. K. Stone, and R. Kishony. 2016. Multidrug evolutionary strategies to reverse antibiotic resistance. Science 351:aad3292.

Beceiro, A., M. Tomás, and G. Bou. 2013. Antimicrobial resistance and virulence: a successful or deleterious association in the bacterial world? Clinical Microbiology Reviews 26:185–230.

Blanquart, F., S. Lehtinen, M. Lipsitch, and C. Fraser. 2018. The evolution of antibiotic resistance in a structured host population. Journal of the Royal Society Interface 15:20180040.

Bolzoni, L., and G. A. De Leo. 2013. Unexpected consequences of culling on the eradication of wildlife diseases: the role of virulence evolution. American Naturalist 181:301–313.

Boots, M., and R. G. Bowers. 2004. The evolution of resistance through costly acquired immunity. Proceedings of the Royal Society B 271:715–723.

Boots, M., and Y. Haraguchi. 1999. The evolution of costly resistance in host-parasite systems. American Naturalist 153:359–370.

Brodin, T., and F. Johansson. 2004. Conflicting selection pressures on the growth/predation-risk trade-off in a damselfly. Ecology 85:2927–2932.

Bull, J. J. 1994. Virulence. Evolution 48:1423–1437.

Bull, J. J., C. S. Vegge, M. Schmerer, W. N. Chaudhry, and B. R. Levin. 2014. Phenotypic resistance and the dynamics of bacterial escape from phage control. PLoS ONE 9:e94690.

Burmeister, A. R., E. Hansen, J. J. Cunningham, E. H. Rego, P. E. Turner, J. S. Weitz, and M. E. Hochberg. 2021. Fighting microbial pathogens by integrating host ecosystem interactions and evolution. Bioessays 43:2000272.

Castle, M. D., and C. A. Gilligan. 2012. An epidemiological framework for modelling fungicide dynamics and control. PLoS ONE 7:e40941.

Chan, B. K., M. Sistrom, J. E. Wertz, K. E. Kortright, D. Narayan, and P. E. Turner. 2016. Phage selection restores antibiotic sensitivity in MDR *Pseudomonas aeruginosa*. Scientific Reports 6:26717.

Chan, B. K., P. E. Turner, S. Kim, H. R. Mojibian, J. A. Elefteriades, and D. Narayan. 2018. Phage treatment of an aortic graft infected with *Pseudomonas aeruginosa*. Evolution, Medicine, and Public Health 2018:60–66.

Chebotar, I. V., M. A. Emelyanova, J. A. Bocharova, N. A. Mayansky, E. E. Kopantseva, and V. M. Mikhailovich. 2021. The classification of bacterial survival strategies in the presence of antimicrobials. Microbial Pathogenesis 155:104901.

Chiarelli, A., N. Cabanel, I. Rosinski-Chupin, P. D. Zongo, T. Naas, R. A. Bonnin, and P. Glaser. 2020. Diversity of mucoid to non-mucoid switch among carbapenemase-producing *Klebsiella pneumoniae*. BMC Microbiology 20:325.

Chisholm, R. H., T. Lorenzi, L. Desvillettes, and B. D. Hughes. 2016. Evolutionary dynamics of phenotype-structured populations: from individual-level mechanisms to population-level consequences. Zeitschrift für angewandte Mathematik und Physik 67:100.

Cokol, M., H. N. Chua, M. Tasan, B. Mutlu, Z. B. Weinstein, Y. Suzuki, M. E. Nergiz, et al. 2011. Systematic exploration of synergistic drug pairs. Molecular Systems Biology 7:544.

REX Consortium. 2010. The skill and style to model the evolution of resistance to pesticides and drugs. Evolutionary Applications 3:375–390.

Copin, R., W. E. Sause, Y. Fulmer, D. Balasubramanian, S. Dyzenhaus, J. M. Ahmed, K. Kumar, et al. 2019. Sequential evolution of virulence and resistance during clonal spread of community-acquired methicillin-resistant *Staphylococcus aureus*. Proceedings of the National Academy of Sciences of the USA 116:1745–1754.

Corwin, J. A., and D. J. Kliebenstein. 2017. Quantitative resistance: more than just perception of a pathogen. Plant Cell 29:655–665.

Costerton, J. W., P. S. Stewart, and E. P. Greenberg. 1999. Bacterial biofilms: a common cause of persistent infections. Science 284: 1318–1322.

Coyne, A. J. K., K. Stamper, R. Kebriaei, D. J. Holger, A. El Ghali, T. Morrisette, B. Biswas, et al. 2022. Phage cocktails with daptomycin and ampicillin eradicates biofilm-embedded multidrug-resistant *Enterococcus faecium* with preserved phage susceptibility. Antibiotics 11:1175.

Cunniffe, N. J., and C. A. Gilligan. 2010. Invasion, persistence and control in epidemic models for plant pathogens: the effect of host demography. Journal of the Royal Society Interface 7:439–451.

Cunniffe, N. J., B. Koskella, C. J. E. Metcalf, S. Parnell, T. R. Gottwald, and C. A. Gilligan. 2015. Thirteen challenges in modelling plant diseases. Epidemics 10:6–10.

Day, T., and S. Gandon. 2006. Insights from Price's equation into evolutionary. Disease Evolution 71:23.

Day, T., D. A. Kennedy, A. F. Read, and D. McAdams. 2021. The economics of managing evolution. PLoS Biology 19:e3001409.

Day, T., T. Parsons, A. Lambert, and S. Gandon. 2020. The price equation and evolutionary epidemiology. Philosophical Transactions of the Royal Society B 375:20190357.

Day, T., and S. R. Proulx. 2004. A general theory for the evolutionary dynamics of virulence. American Naturalist 163:E40–E63.

Dewachter, L., M. Fauvart, and J. Michiels. 2019. Bacterial heterogeneity and antibiotic survival: understanding and combatting persistence and heteroresistance. Molecular Cell 76:255–267.

Dutta, A., D. Croll, B. A. McDonald, and L. G. Barrett. 2020. Maintenance of variation in virulence and reproduction in populations of an agricultural plant pathogen. bioRxiv, https://doi.org/10.1101/2020.04.15.043208.

Elderfield, J. A., F. J. Lopez-Ruiz, F. van den Bosch, and N. J. Cunniffe. 2018. Using epidemiological principles to explain fungicide resistance management tactics: why do mixtures outperform alternations? Phytopathology 108:803–817.

El Meouche, I., and M. J. Dunlop. 2018. Heterogeneity in efflux pump expression predisposes antibiotic-resistant cells to mutation. Science 362:686–690.

Esteves, N. C., and B. E. Scharf. 2022. Flagellotropic bacteriophages: opportunities and challenges for antimicrobial applications. International Journal of Molecular Sciences 23:7084.

Fanning, S., and A. P. Mitchell. 2012. Fungal biofilms. PLoS Pathogens 8:e1002585.

Feng, Y., C. C. Tonon, S. Ashraf, and T. Hasan. 2021. Photodynamic and antibiotic therapy in combination against bacterial infections: efficacy, determinants, mechanisms, and future perspectives. Advanced Drug Delivery Reviews 177:113941.

Fernandes, R. L., M. Nierychlo, L. Lundin, A. E. Pedersen, P. P. Tellez, A. Dutta, M. Carlquist, et al. 2011. Experimental methods and modeling techniques for description of cell population heterogeneity. Biotechnology Advances 29:575–599.

Forster, G. A., and C. A. Gilligan. 2007. Optimizing the control of disease infestations at the landscape scale. Proceedings of the National Academy of Sciences of the USA 104:4984–4989.

Foster, S. P., I. Denholm, G. Poppy, R. Thompson, and W. Powell. 2011. Fitness trade-off in peach-potato aphids (*Myzus persicae*) between insecticide resistance and vulnerability to parasitoid attack at several spatial scales. Bulletin of Entomological Research 101:659–666.

Foster, S. P., M. Tomiczek, R. Thompson, I. Denholm, G. Poppy, A. R. Kraaijeveld, and W. Powell. 2007. Behavioural side-effects of insecticide resistance in aphids increase their vulnerability to parasitoid attack. Animal Behaviour 74:621–632.

Frank, S. A. 1996. Models of parasite virulence. Quarterly Review of Biology 71:37–78.

Furusawa, C., T. Horinouchi, and T. Maeda. 2018. Toward prediction and control of antibiotic-resistance evolution. Current Opinion in Biotechnology 54:45–49.

Galvani, A. P. 2003. Epidemiology meets evolutionary ecology. Trends in Ecology and Evolution 18:132–139.

Gandon, S., M. J. Mackinnon, S. Nee, and A. F. Read. 2001. Imperfect vaccines and the evolution of pathogen virulence. Nature 414:751–756.

———. 2003. Imperfect vaccination: some epidemiological and evolutionary consequences. Proceedings of the Royal Society B 270:1129–1136.

Gatenby, R. A., J. Brown, and T. Vincent. 2009. Lessons from applied ecology: cancer control using an evolutionary double bind. Cancer Research 69:7499–7502.

Gefen, O., and N. Q. Balaban. 2009. The importance of being persistent: heterogeneity of bacterial populations under antibiotic stress. FEMS Microbiology Reviews 33:704–717.

Gilligan, C. A. 2002. An epidemiological framework for disease management. Advances in Botanical Research 38:1–64.

Gilligan, C. A., and F. van den Bosch. 2008. Epidemiological models for invasion and persistence of pathogens. Annual Review of Phytopathology 46:385–418.

Giraud, E., I. Rychlik, and A. Cloeckaert. 2017. Antimicrobial resistance and virulence common mechanisms. Frontiers in Microbiology 8:310.

González, R., A. Butković, and S. F. Elena. 2019. Role of host genetic diversity for susceptibility-to-infection in the evolution of virulence of a plant virus. Virus Evolution 5:vez024.

Gotthard, K. 2000. Increased risk of predation as a cost of high growth rate: an experimental test in a butterfly: predation as a cost of high growth rate. Journal of Animal Ecology 69:896–902.

Gu Liu, C., S. I. Green, L. Min, J. R. Clark, K. C. Salazar, A. L. Terwilliger, H. B. Kaplan, B. W. Trautner, R. F. Ramig, and A. W. Maresso. 2020. Phage-antibiotic synergy is driven by a unique combination of antibacterial mechanism of action and stoichiometry. MBio 11:e01462-20.

Gurney, J., L. Pradier, J. S. Griffin, C. Gougat-Barbera, B. K. Chan, P. E. Turner, O. Kaltz, and M. E. Hochberg. 2020. Phage steering of antibiotic-resistance evolution in the bacterial pathogen, *Pseudomonas aeruginosa*. Evolution, Medicine, and Public Health 2020:148–157.

Hall, R. J., S. Gubbins, and C. A. Gilligan. 2004. Invasion of drug and pesticide resistance is determined by a trade-off between treatment efficacy and relative fitness. Bulletin of Mathematical Biology 66:825–840.

Hawkins, N., and B. Fraaije. 2018. Fitness penalties in the evolution of fungicide resistance. Annual Review of Phytopathology 56:339–360.

Hethcote, H. W. 2000. The mathematics of infectious diseases. SIAM Review 42:599–653.

Hewitt, S. K., D. S. Foster, P. S. Dyer, and S. V. Avery. 2016. Phenotypic heterogeneity in fungi: importance and methodology. Fungal Biology Reviews 30:176–184.

Kebriaei, R., K. L. Lev, R. M. Shah, K. C. Stamper, D. J. Holger, T. Morrisette, A. J. Kunz Coyne, S. M. Lehman, and M. J. Rybak. 2022. Eradication of biofilm-mediated methicillin-resistant *Staphylococcus aureus* infections in vitro: bacteriophage-antibiotic combination. Microbiology Spectrum 10:e00411-22.

Keeling, M. J., and P. Rohani. 2011. Modeling infectious diseases in humans and animals. Princeton University Press, Princeton, NJ.

Kennedy, M. C., E. D. Ford, P. Singleton, M. Finney, and J. K. Agee. 2008. Informed multi-objective decision-making in environmental management using Pareto optimality. Journal of Applied Ecology 45:181–192.

Kimura, M. 1965. A stochastic model concerning the maintenance of genetic variability in quantitative characters. Proceedings of the National Academy of Sciences of the USA 54:731–736.

Korobeinikov, A. 2018. Immune response and within-host viral evolution: immune response can accelerate evolution. Journal of Theoretical Biology 456:74–83.

Korobeinikov, A., and G. C. Wake. 2002. Lyapunov functions and global stability for SIR, SIRS, and SIS epidemiological models. Applied Mathematics Letters 15:955–960.

Lacey, L., D. Grzywacz, D. Shapiro-Ilan, R. Frutos, M. Brownbridge, and M. Goettel. 2015. Insect pathogens as biological control agents: back to the future. Journal of Invertebrate Pathology 132:1–41.

Lafferty, K. D., G. DeLeo, C. J. Briggs, A. P. Dobson, T. Gross, and A. M. Kuris. 2015. A general consumer-resource population model. Science 349:854–857.

Laine, A.-L., and B. Barrès. 2013. Epidemiological and evolutionary consequences of life-history trade-offs in pathogens. Plant Pathology 62:96–105.

Lässig, M., V. Mustonen, and A. M. Walczak. 2017. Predicting evolution. Nature Ecology and Evolution 1:0077.

Laure, N. N., and J. Ahn. 2022. Phage resistance-mediated tradeoffs with antibiotic resistance in *Salmonella typhimurium*. Microbial Pathogenesis 171:105732.

Lázár, V., A. Martins, R. Spohn, L. Daruka, G. Grézal, G. Fekete, M. Számel, et al. 2018. Antibiotic-resistant bacteria show widespread collateral sensitivity to antimicrobial peptides. Nature Microbiology 3:718–731.

Lázár, V., G. Pal Singh, R. Spohn, I. Nagy, B. Horváth, M. Hrtyan, R. Busa-Fekete, et al. 2013. Bacterial evolution of antibiotic hypersensitivity. Molecular Systems Biology 9:700.

Lehtinen, S., F. Blanquart, M. Lipsitch, C. Fraser; Maela Pneumococcal Collaboration. 2019. On the evolutionary ecology of multidrug resistance in bacteria. PLoS Pathogens 15:e1007763.

Lenski, R. E. 1998. Bacterial evolution and the cost of antibiotic resistance. International Microbiology 1:265–270.

Levin, B. R., and K. I. Udekwu. 2010. Population dynamics of antibiotic treatment: a mathematical model and hypotheses for time-kill and continuous-culture experiments. Antimicrobial Agents and Chemotherapy 54:3414–3426.

Lima, G., F. De Curtis, D. Piedimonte, A. M. Spina, and V. De Cicco. 2006. Integration of biocontrol yeast and thiabendazole protects stored apples from fungicide sensitive and resistant isolates of *Botrytis cinerea*. Postharvest Biology and Technology 40:301–307.

Lion, S. 2018. Theoretical approaches in evolutionary ecology: environmental feedback as a unifying perspective. American Naturalist 191:21–44.

Lorenzi, T., R. H. Chisholm, and J. Clairambault. 2016. Tracking the evolution of cancer cell populations through the mathematical lens of phenotype-structured equations. Biology Direct 11:43.

Lyu, Z., A. Yang, P. Villanueva, A. Singh, and J. Ling. 2021. Heterogeneous flagellar expression in single salmonella cells promotes diversity in antibiotic tolerance. MBio 12:e02374-21.

Maeda, T., J. Iwasawa, H. Kotani, N. Sakata, M. Kawada, T. Horinouchi, A. Sakai, K. Tanabe, and C. Furusawa. 2020. High-throughput laboratory evolution reveals evolutionary constraints in *Escherichia coli*. Nature Communications 11:5970.

Maltas, J., and K. B. Wood. 2019. Pervasive and diverse collateral sensitivity profiles inform optimal strategies to limit antibiotic resistance. PLoS Biology 17:e3000515.

Mangalea, M. R., and B. A. Duerkop. 2020. Fitness trade-offs resulting from bacteriophage resistance potentiate synergistic antibacterial strategies. Infection and Immunity 88:e00926-19.

Martinez, J. L., M. B. Sánchez, L. Martínez-Solano, A. Hernandez, L. Garmendia, A. Fajardo, and C. Alvarez-Ortega. 2009. Functional role of bacterial multidrug efflux pumps in microbial natural ecosystems. FEMS Microbiology Reviews 33:430–449.

Martínez, S. R., Y. B. Palacios, D. A. Heredia, M. L. Agazzi, and A. M. Durantini. 2019. Phenotypic resistance in photodynamic inactivation unravelled at the single bacterium level. ACS Infectious Diseases 5:1624–1633.

Mattei, M., L. Frunzo, B. D'acunto, Y. Pechaud, F. Pirozzi, and G. Esposito. 2018. Continuum and discrete approach in modeling biofilm development and structure: a review. Journal of Mathematical Biology 76:945–1003.

McLeod, D. V., and S. Gandon. 2021. Understanding the evolution of multiple drug resistance in structured populations. eLife 10: e65645.

Meaden, S., K. Paszkiewicz, and B. Koskella. 2015. The cost of phage resistance in a plant pathogenic bacterium is context-dependent. Evolution 69:1321–1328.

Medina-Pastor, P., and G. Triacchini. 2020. The 2018 European Union report on pesticide residues in food. EFSA Journal 18:6057.

Miele, L., R. Evans, and S. Azaele. 2021. Redundancy-selection trade-off in phenotype-structured populations. Journal of Theoretical Biology 531:110884.

Miele, L., R. M. L. Evans, N. J. Cunniffe, C. Torres-Barceló, and D. Bevacqua. 2023. Code from: Evolutionary epidemiology consequences of trait-dependent control of heterogeneous parasites. American Naturalist, Zenodo, https://doi.org/10.5281/zenodo.7874696.

Mohiuddin, S. G., P. Kavousi, and M. A. Orman. 2020. Flow-cytometry analysis reveals persister resuscitation characteristics. BMC Microbiology 20:202.

Montarry, J., R. Corbiere, S. Lesueur, I. Glais, and D. Andrivon. 2006. Does selection by resistant hosts trigger local adaptation in plant–pathogen systems? Journal of Evolutionary Biology 19:522–531.

Munita, J. M., and C. A. Arias. 2016. Mechanisms of antibiotic resistance. Microbiology Spectrum 4:10.1128/microbiolspec.vmbf-0016-2015.

Nelson, P., and G. May. 2020. Defensive symbiosis and the evolution of virulence. American Naturalist 196:333–343.

Ney, B., M.-O. Bancal, P. Bancal, I. Bingham, J. Foulkes, D. Gouache, N. Paveley, and J. Smith. 2013. Crop architecture and crop tolerance to fungal diseases and insect herbivory: mechanisms to limit crop losses. European Journal of Plant Pathology 135:561–580.

Nichol, D., J. Rutter, C. Bryant, A. M. Hujer, S. Lek, M. D. Adams, P. Jeavons, A. R. Anderson, R. A. Bonomo, and J. G. Scott. 2019. Antibiotic collateral sensitivity is contingent on the repeatability of evolution. Nature Communications 10:334.

Nunes, I., S. Jacquiod, A. Brejnrod, P. E. Holm, A. Johansen, K. K. Brandt, A. Priemé, and S. J. Sørensen. 2016. Coping with copper: legacy effect of copper on potential activity of soil bacteria following a century of exposure. FEMS Microbiology Ecology 92: fiw175.

Okusu, H., D. Ma, and H. Nikaido. 1996. AcrAB efflux pump plays a major role in the antibiotic resistance phenotype of *Escherichia coli* multiple-antibiotic-resistance (Mar) mutants. Journal of Bacteriology 178:306–308.

Ons, L., D. Bylemans, K. Thevissen, and B. P. Cammue. 2020. Combining biocontrol agents with chemical fungicides for integrated plant fungal disease control. *Microorganisms* 8:1930.

Pál, C., B. Papp, and V. Lázár. 2015. Collateral sensitivity of antibiotic-resistant microbes. Trends in Microbiology 23:401–407.

Palmer, A. C., and R. Kishony. 2013. Understanding, predicting and manipulating the genotypic evolution of antibiotic resistance. Nature Reviews Genetics 14:243–248.

Patyka, V., N. Buletsa, L. Pasichnyk, N. Zhitkevich, A. Kalinichenko, T. Gnatiuk, and L. Butsenko. 2016. Specifics of pesticides effects on the phytopathogenic bacteria. Ecological Chemistry and Engineering S 23:311–331.

Paveley, N., R. Sylvester-Bradley, R. Scott, J. Craigon, and W. Day. 2001. Steps in predicting the relationship of yield on fungicide dose. Phytopathology 91:708–716.

Perrier, A., X. Barlet, D. Rengel, P. Prior, S. Poussier, S. Genin, and A. Guidot. 2019. Spontaneous mutations in a regulatory gene induce phenotypic heterogeneity and adaptation of *Ralstonia solanacearum* to changing environments. Environmental Microbiology 21:3140–3152.

Perry, G. H. 2021. Evolutionary medicine. eLife 10:e69398.

Pinheiro, F., O. Warsi, D. I. Andersson, and M. Lässig. 2021. Metabolic fitness landscapes predict the evolution of antibiotic resistance. Nature Ecology and Evolution 5:677–687.

Porco, T. C., J. O. Lloyd-Smith, K. L. Gross, and A. P. Galvani. 2005. The effect of treatment on pathogen virulence. Journal of Theoretical Biology 233:91–102.

Rezzoagli, C., M. Archetti, I. Mignot, M. Baumgartner, and R. Kümmerli. 2020. Combining antibiotics with antivirulence compounds can have synergistic effects and reverse selection for antibiotic resistance in *Pseudomonas aeruginosa*. PLoS Biology 18:e3000805.

Rimbaud, L., J. Papaïx, J.-F. Rey, L. G. Barrett, and P. H. Thrall. 2018. Assessing the durability and efficiency of landscape-based strategies to deploy plant resistance to pathogens. PLoS Computational Biology 14:e1006067.

Rodriguez-Gonzalez, R. A., C. Y. Leung, B. K. Chan, P. E. Turner, and J. S. Weitz. 2020. Quantitative models of phage-antibiotic combination therapy. MSystems 5:e00756-19.

Roemhild, R., and D. I. Andersson. 2021. Mechanisms and therapeutic potential of collateral sensitivity to antibiotics. PLoS Pathogens 17:e1009172.

Ryan, R. P., D. J. Ryan, Y.-C. Sun, F.-M. Li, Y. Wang, and D. N. Dowling. 2007. An acquired efflux system is responsible for copper resistance in *Xanthomonas* strain IG-8 isolated from China. FEMS Microbiology Letters 268:40–46.

Sacristán, S., and F. García-Arenal. 2008. The evolution of virulence and pathogenicity in plant pathogen populations. Molecular Plant Pathology 9:369–384.

Sasaki, A., S. Lion, and M. Boots. 2022. Antigenic escape selects for the evolution of higher pathogen transmission and virulence. Nature Ecology and Evolution 6:51–62.

Saubin, M., C. Louet, L. Bousset, F. Fabre, P. Frey, I. Fudal, F. Grognard, et al. 2023. Improving sustainable crop protection using population genetics concepts. Molecular Ecology 32:2461–2471.

Schröter, L., and P. Dersch. 2019. Phenotypic diversification of microbial pathogens—cooperating and preparing for the future. Journal of Molecular Biology 431:4645–4655.

Schuster, P., and K. Sigmund. 1983. Replicator dynamics. Journal of Theoretical Biology 100:533–538.

Shoval, O., H. Sheftel, G. Shinar, Y. Hart, O. Ramote, A. Mayo, E. Dekel, K. Kavanagh, and U. Alon. 2012. Evolutionary trade-offs, Pareto optimality, and the geometry of phenotype space. Science 336:1157–1160.

Song, L., X. Yang, J. Huang, X. Zhu, G. Han, Y. Wan, Y. Xu, G. Luan, and X. Jia. 2021. Phage selective pressure reduces virulence of hypervirulent *Klebsiella pneumoniae* through mutation of the *wzc* gene. Frontiers in Microbiology 12:739319.

Stearns, S. C. 2012. Evolutionary medicine: its scope, interest and potential. Proceedings of the Royal Society B 279:4305–4321.

Stoks, R., M. D. Block, F. Van De Meutter, and F. Johansson. 2005. Predation cost of rapid growth: behavioural coupling and physiological decoupling. Journal of Animal Ecology 74:708–715.

Strobbe, F., M. A. McPeek, M. De Block, and R. Stoks. 2011. Fish predation selects for reduced foraging activity. Behavioral Ecology and Sociobiology 65:241–247.

Suzuki, S., T. Horinouchi, and C. Furusawa. 2014. Prediction of antibiotic resistance by gene expression profiles. Nature Communications 5:5792.

Taber, H. W., J. P. Mueller, P. F. Miller, and A. Arrow. 1987. Bacterial uptake of aminoglycoside antibiotics. Microbiological Reviews 51:439–457.

Tamm, L., I. Pertot, A. Schmitt, V. Verrastro, J. Magid, E. Bünemann, K. Möller, et al. 2018. Replacement of contentious inputs in organic farming systems (RELACS)—a comprehensive horizon 2020 project. Page 47 *in* Book of abstracts. Sixth International Conference on Organic Agriculture Sciences (ICOAS), November 7–9 , 2018, Eisenstadt, Austria.

Taylor, N., and N. Cunniffe. 2022. Modelling quantitative fungicide resistance and breakdown of resistant cultivars: designing integrated disease management strategies for *Septoria* of winter wheat. bioRxiv, https://doi.org/10.1101/2022.08.10.503500.

Tits, J., B. P. Cammue, and K. Thevissen. 2020. Combination therapy to treat fungal biofilm-based infections. International Journal of Molecular Sciences 21:8873.

Torres-Barceló, C., and Hochberg, M. E. 2016. Evolutionary rationale for phages as complements of antibiotics. Trends in Microbiology 24:249–256.

van den Bosch, F., and C. A. Gilligan. 2008. Models of fungicide resistance dynamics. Annual Review of Phytopathology 46:123–147.

van den Bosch, F., N. Paveley, F. van den Berg, P. Hobbelen, and R. Oliver. 2014. Mixtures as a fungicide resistance management tactic. Phytopathology 104:1264–1273.

Van Emden, H. F., and R. Harrington. 2017. Aphids as crop pests. CABI, Wallingford.

Vincent, B. M., A. K. Lancaster, R. Scherz-Shouval, L. Whitesell, and S. Lindquist. 2013. Fitness trade-offs restrict the evolution of resistance to amphotericin B. PLoS Biology 11:e1001692.

Vyska, M., N. Cunniffe, and C. Gilligan. 2016. Trade-off between disease resistance and crop yield: a landscape-scale mathematical modelling perspective. Journal of the Royal Society Interface 13:20160451.

Walter, A., and S. Lion. 2021. Epidemiological and evolutionary consequences of periodicity in treatment coverage. Proceedings of the Royal Society B 288:20203007.

Weigel, W., and P. Dersch. 2018. Phenotypic heterogeneity: a bacterial virulence strategy. Microbes and Infection 20:570–577.

Weiße, A. Y., D. A. Oyarzún, V. Danos, and P. S. Swain. 2015. Mechanistic links between cellular trade-offs, gene expression, and growth. Proceedings of the National Academy of Sciences of the USA 112:E1038–E1047.

Werner, E., and B. Anholt. 1993. Ecological consequences of the trade-off between growth and mortality rates mediated by foraging activity. American Naturalist 142:242–272.

WHO (World Health Organization). 2014. Antimicrobial resistance global report on surveillance: 2014 summary. Technical report, WHO.

Zhan, J., P. H. Thrall, J. Papaïx, L. Xie, and J. J. Burdon. 2015. Playing on a pathogen's weakness: using evolution to guide sustainable plant disease control strategies. Annual Review of Phytopathology 53:19–43.

Zurita-Gutiérrez, Y. H., and S. Lion. 2015. Spatial structure, host heterogeneity and parasite virulence: implications for vaccine-driven evolution. Ecology Letters 18:779–789.

Associate Editor: Matthew J. Ferrari
Editor: Erol Akçay

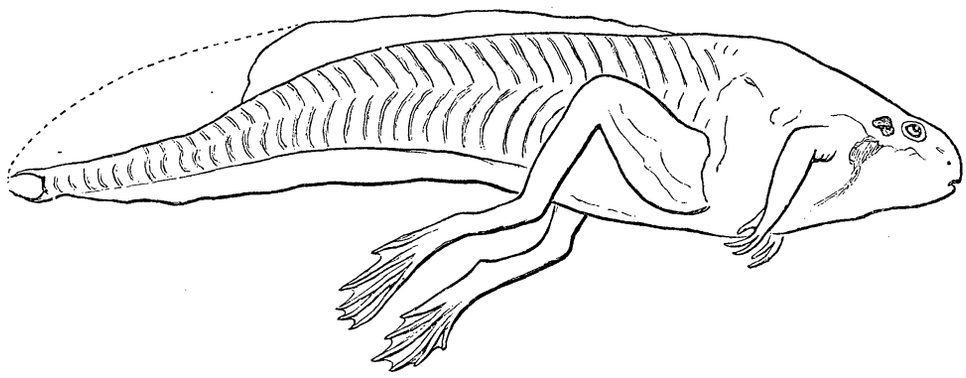

"Then we should notice the beginning of segmentation, its progress, and the successful changes of form in the embryo, until it tears the shell, and with great, wondering eyes stares out upon its watery world a tadpole." From "Pseudis, 'The Paradoxical Frog,'" by S. W. Garman (*The American Naturalist*, 1877, 11:587–591).